Cement & Concrete Composites 21 (1999) 391–401

Cement & Concrete Composites

Resistance of fibre concrete slabs to low velocity projectile impact

K.C.G. Ong *, M. Basheerkhan, P. Paramasivam

Department of Civil Engineering, Centre for Construction Materials and Technology, National University of Singapore, 119260 Singapore, Singapore

Received 3 November 1998; accepted 21 July 1999

Abstract

An investigation on fibre concrete slabs subjected to low velocity projectile impact was carried out to assess impact resistance. The main variables of the study were type of fibre and volume fraction of fibres. The types of fibres chosen were polyolefin, polyvinyl alcohol and steel. The volume fraction of fibres examined were 0%, 1% and 2%. A total of 10 square slabs of size 1 m and 50 mm thickness were cast and tested. Impact was achieved by dropping projectile of mass 43 kg from a height of 4 m, by means of an instrumented impact test facility. Test results indicate that hooked-end steel fibre concrete slabs have better cracking and energy absorption characteristics than slabs reinforced with other fibre types. Slabs reinforced with polyvinyl alcohol fibres exhibited higher fracture energy values compared to slabs reinforced with polyolefin fibres. © 1999 Elsevier Science Ltd. All rights reserved.

Keywords: Fibre concrete; Slab; Impact; Projectile; Steel; Polyolefin; Polyvinyl alcohol

1. Introduction

Fibre reinforced concrete is widely used in many structural and non-structural applications, e.g., airport runways, slabs on grade, shotcrete for slope and tunnel stabilisation, pre-cast concrete products, coastal structures, machine foundations, defence shelters, etc. Worldwide usage of this composite is presently reported [1] at 150,000 metric tonnes annually. It has been reported that adding fibres to concrete increased its toughness and impact resistance among many of its other engineering properties. Different types of fibres from natural to metallic and polymeric are being used [2–4].

Use of steel fibres has certain associated problems that are yet to be resolved. Steel fibres present in close proximity to the surface of concrete are prone to corrosion and hence brown spots appear on the concrete surface after sometime. Interest in the use of polymeric fibres is fairly recent. Owing to the inert and non-corrosive nature of the polymeric materials, they are eminently suitable for use in chemically aggressive environments such as concrete lining for septic tanks, coastal structures, and structures in a hot and wet tropical climate.

Apart from the usual static loading and other types of dynamic loading, concrete structures may also be subjected to impact loads during their life span [5]. This might be due to tornado-generated projectiles, aircraft crashes, fragments of failed turbines and pipe work, and accidental drop-weights. Impact loading of structural members involves a complex process where both structural and material parameters can influence their performance. In an attempt to address the problems associated with impact loading, numerous research programmes have been undertaken leading to the development of various test methods.

ACI Committee 544 [6] proposed a repeated drop-weight testing apparatus for testing fibre concrete materials. In this test, a 4.5 kg (10 lb) steel ball is dropped repeatedly through a height of 457 mm (18 in.) onto a standard concrete disc type specimen. The concrete specimens used are 63.4 mm (2.5 in.) thick and 152 mm (6 in.) in diameter. The steel ball is dropped consecutively, and the number of blows causing the first visible crack on the impact surface and ultimate failure of the disc specimen recorded. This technique has been used to compare the relative improvements in impact resistance of different fibre concrete mixes [6,7] including fibre reinforced lightweight concrete [8].

A rotating impact machine used generally for investigating metal specimens has also been used to conduct tests on fibre reinforced cement concretes [9].

* Corresponding author.

PII: S0958-9465(99)00024-4

The high strain rate behaviour of cement composites in uniaxial tension and compression has been studied using the split Hopkinson bar test [10,11]. Another test, the Charpy impact test, originally recommended for metals, has also been employed to evaluate impact performance in terms of the energy absorption capacity of steel fibre reinforced concrete [12,13]. The modified instrumented Charpy impact test developed by Gopalaratnam et al. [14] has been used for studying impact behaviour of steel and glass fibre reinforced cement composites. Ito et al. [15] used a compressed air-gun facility to study the impact resistance and residual strength of pre-stressed concrete beams. Various instrumented drop-weight impact test set-ups to investigate the effect of impact loading on fibre reinforced concrete have also been reported [16–18].

Most instrumented experimental investigations are performed using drop-weight systems, servo-hydraulic rams, or pendulums where high energy levels are achieved by using large masses at relatively low impact velocities. These impact velocities, of the order of a few metres per second, are chosen because of ease of instrumentation when compared to experiments involving higher velocities. Very high strain rates could be achieved even under low velocity impact tests by proper choice of the dimensions of the test specimens. Thus most impact test methods reported in available literature are based on low velocity tests. A review of the various available methods for impact testing can be found in the literature [19,20]. Impact tests at high velocities are generally carried out with non-instrumented projectiles.

Impact can be classified as soft or hard. When the projectile deformability is large compared to the target deformability the impact is said to be 'soft', and if the projectile deformability is relatively small the impact is termed 'hard'. In this study hard projectile impact is considered and this type of impact results in local damage and also in overall dynamic response in the form of flexural deformation. Local damage consists of spalling of concrete at the impact face and scabbing of concrete at the rear face together with projectile penetration into the target. Overall dynamic response of the target consists of flexural deformations resulting in flexural or shear failure. Under impact situations the material is required to absorb a large amount of energy within a short duration. Under these circumstances, quantifying the amount of energy that is needed to cause a considerable amount of damage to the material is a very important requirement for qualitative and quantitative studies on any material.

This paper describes the effectiveness of fibre concrete slabs containing polymeric (straight polyolefin and straight polyvinyl alcohol) and metallic (hooked-end steel) fibres subjected to low velocity impact loading. In the present study slab specimens 1 m^2 in size and thickness 30 mm were used. The impact was achieved by dropping a projectile of mass 43 kg from a height of 4 m, by means of an instrumented impact test facility. The results obtained in this study are specific to the size of specimen tested, the boundary conditions and the test configuration adopted.

2. Experimental program

2.1. Materials used

The materials used were ordinary Portland cement, natural sand and crushed granite aggregates of maximum size 10 mm. The mix proportion of cement:sand:coarse aggregate used was 1:1.3:2.1 by weight with a water–cement ratio of 0.4. The three types of fibres used were straight polyolefin, kuralon-cut polyvinyl alcohol (PVA) and hooked-end steel fibres. The properties of the fibres are summarised in Table 1. A sulphonated napthalene-based superplasticizer was added at the rate of 7.5 cc/kg of cement in order to improve the workability of fibre concrete mixes.

2.2. Test specimens

The parameters investigated were the type and volume fraction of fibres. The types of fibres used were straight polyolefin, polyvinyl alcohol and hooked-end steel fibres. The volume fraction of fibres was varied as 0%, 0.5%, 1% and 2%. All the slabs were square, of size 1 m and thickness 50 mm. A total of 10 specimens were cast and tested. The details of the test specimens are given in Table 2. The designation of slabs is explained as follows. PC is a plain concrete slab. The alphabets represent the type of fibre used in the slab and the numerals represent the volume fraction of fibres present. Hence, POFC, PVAFC and SFC stand for polyolefin, PVA and steel fibre reinforced concrete slab, respectively. The numerals 05, 10 and 20 represent 0.5%, 1.0% and 2.0% volume fraction of fibres, respectively. For example, POFC05 indicates a polyolefin fibre concrete slab containing 0.5% volume fraction of fibres.

Cement, aggregates and water were mixed thoroughly in a rotary mixer. The fibres were added manually during mixing and care was taken to avoid balling of fibres. When fibres were used, the required amount of superplasticizer was premixed with water. Wooden moulds were used for casting the slabs. A table vibrator was used to achieve proper compaction. Three 100 mm cubes were also cast for each batch to determine the compressive strength of the mix. The slabs were demoulded after 24 h and moist cured for 28 days. They were then air dried in the laboratory until testing.

Table 1
Properties of fibres used

Fibre type	Shape	Length (mm)	Diameter (mm)	Tensile strength (MPa)	Modulus of elasticity (GPa)
Polyolefin	Straight	50	0.63	275	2.65
Polyvinyl alcohol	Straight	12	0.2	900	29
Steel	Hooked-end	30	0.5	1275	200

Table 2
Details of test specimens

Slab designation	Type of fibre	Volume fraction of fibre (%)
PC	–	0
POFC05	Polyolefin	0.5
POFC10	Polyolefin	1.0
POFC20	Polyolefin	2.0
PVAFC05	Polyvinyl alcohol	0.5
PVAFC10	Polyvinyl alcohol	1.0
PVAFC20	Polyvinyl alcohol	2.0
SFC05	Steel	0.5
SFC10	Steel	1.0
SFC20	Steel	2.0

2.3. Test procedure

The drop-weight impact test set-up used is shown in Fig. 1. It consisted of two square steel frames between which the slab to be tested was clamped to prevent bouncing of the slab away from the support upon and after impact. The slab was simply supported on all four sides by means of 20 mm diameter continuous steel bars welded to both the frames. All the slabs were simply supported over a span of 900 mm in both directions. The bottom frame was welded and supported on rigid columns. A central impact was achieved by means of a guide. The guide in the form of a square was fabricated using aluminium angles in which the projectile was allowed to slide freely up and down. A manually operated winch was used to lift the projectile to the required height. Grease was applied on the rollers to reduce friction along the guides and to ensure a controlled and smooth fall. It has been observed that friction between the guide pillars and the hammer may reduce the acceleration of the hammer during free fall below the earth's gravitational acceleration of 9.81 m/s [2,21]. In the tests carried out, all slabs were subjected to impact by a hemi-spherical nose shaped projectile of mass 43 kg dropped from a height of 4 m.

A schematic diagram of the instrumentation and the data acquisition system is presented in Fig. 2. The projectile was instrumented with an accelerometer to measure the impact load. The deceleration of the projectile multiplied by the mass of the projectile gives a measure of the applied impact load. Accelerometers attached to the slab were used to determine the deflection of the slab. The accelerations were measured on the top surface of the slabs at 150 and 300 mm away from centre of the slab. A digital circuit in combination with laser emitters and photodiodes designed to determine the incident and rebound velocities of the projectile was used to trigger the data acquisition system. When the projectile crosses

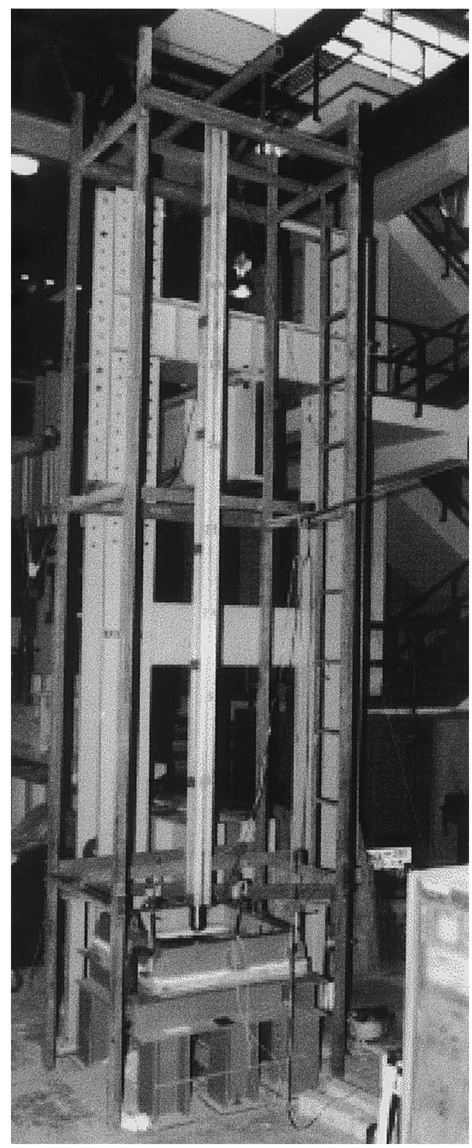

Fig. 1. Drop-weight impact test set-up.

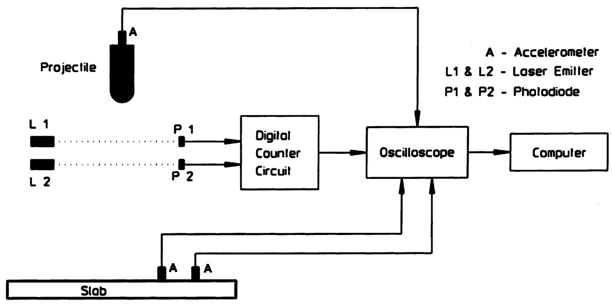

Fig. 2. Schematic diagram of instrumentation and data acquisition system.

the second photodiode, the system gets triggered and the data captured over a specified time interval. This capturing period depends on the number of channels and the scan rate specified. A scan rate of 1 MHz per channel was used. A pre-trigger interval was also specified so that no data were lost as acquisition of data proceeds. For data acquisition, a digital oscilloscope was used and the data analysed in a DEC workstation. Under impact testing, electrical noise will occur due to the electronic systems used and the mechanical system adopted. Any physical measurement of acceleration or force under these conditions is accompanied by random noise of very high frequencies. In the present case, a filtering frequency of 5 kHz was used. This was arrived at by analysing the frequency content of the measured signal using a FFT routine [25]. The recorded signals were digitally filtered using a low-pass second-order Butterworth filter.

3. Method of analysis 22

It has been well established that due to the specimen inertial effects under high rates of loading [20–23], the experimentally observed load, $P_o(t)$, is not the true bending load, $P_b(t)$. Since cement-based materials are usually brittle, the true bending load may only be a fraction of the experimentally observed load. Depending on the rate of loading and the brittleness of the material, a large part of the impact event may occur while the specimen is still being accelerated. The acceleration of the specimen gives rise to inertial force and this force is distributed throughout the specimen. The projectile impact considered here, acts as a concentrated load at the centre of the slab. There are two ways of dealing with the problem of inertial loading: first, by reducing the stiffness of the contact zone [23] and second, by measuring the inertial forces by placing accelerometers on the specimen [21]. In the latter a generalised form of the inertial load is used in correcting the observed load. The virtual work principle [21] is used in calculating the generalised inertial load, $P_i(t)$.

Consider the simply supported slab shown in Fig. 3(a) subjected to a concentrated load at its centre. For this problem, it may be assumed [24,25] that the accelerations, velocities, and displacements at any point in the slab, at any instant of time, t, are sinusoidal along both x- and y-axis (Fig. 3(b)). In order to replace the distributed inertial load in the slab by a generalised inertial load, $P_i(t)$, the virtual work done by all the distributed inertial loads may be equated to the virtual work done by $P_i(t)$ alone. Thus the generalised inertial load, $P_i(t)$, is obtained [26] as

$$P_i(t) = \frac{1}{4}\rho abh\ddot{w}_o(t), \quad (1)$$

where ρ is the density of the slab material, a the length of the slab along x-axis, b the length of the slab along y-axis, h the thickness of the slab and $\ddot{w}_o(t)$ is the acceleration at the centre of the slab at any time, t.

Considering the loads $P_o(t)$, $P_i(t)$ and $P_b(t)$, and idealising the slab impact problem as a single degree of freedom system, the bending load exerted on the slab, $P_b(t)$, can be found using the equation of dynamic equilibrium as

$$P_b(t) = P_o(t) - P_i(t). \quad (2)$$

The bending load obtained above using Eq. (2) may be regarded as an equivalent static load for the purpose of analysis. The displacement at the centre of the slab, $w_o(t)$, was obtained numerically by double integrating the extrapolated acceleration at the slab centre with respect to time. Energy absorbed during the impact

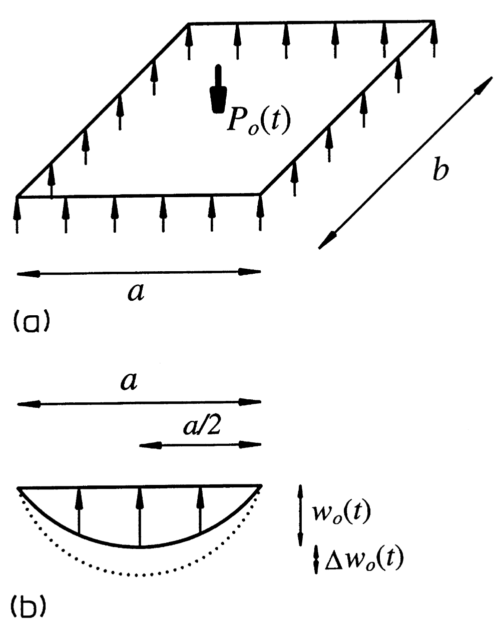

Fig. 3. (a) Simply supported slab under a transverse impact load. (b) Assumed plate deflections and the application of virtual work principle to calculate the generalised inertial load.

event was calculated based on the area under $P_b(t)$ versus $w_o(t)$ curve.

4. Results and discussion

The performance of the slabs containing polyolefin, polyvinyl alcohol and steel with 0.5%, 1% and 2% volume fraction of fibres are discussed in the following sections. All slabs were subjected to single impact by hemi-spherical nose shaped projectile of mass 43 kg dropped from a height of 4 m. The observations are specific only to the size of specimen tested, the boundary conditions and the test configuration adopted.

4.1. Cracking behaviour

The failure of the plain concrete (PC) slab under impact was catastrophic as seen in Fig. 4. The projectile completely perforated the slab with the formation of a frustum-shaped fracture zone and the slab shattered into pieces. The failure of the slab may be envisaged as follows: On striking the slab, the projectile penetrated the slab and during the contact period, very high stresses developed in the vicinity of impact point which led to the formation of shear cone shaped fracture zone. The slab losing integrity and gaining momentum experienced large displacements inducing more damage due to radial crack formation. With 0.5% volume fraction of fibres (Fig. 5), slabs with polyolefin (POFC05) and PVA fibres (PVAFC05) were also perforated by the projectile. However, the slab reinforced with steel fibres (SFC05) was not perforated and suffered less damage. Slabs POFC05 and PVA05 broke into few pieces while slab SFC05 maintained its integrity even after impact. At 1% and 2% volume fraction of fibres, the slabs containing PVA fibres (PVAFC10 & PVAFC20) were perforated by the projectile and also broke into few pieces. Although the polyolefin fibre reinforced slab (POFC10) suffered damage similar to PVAFC10 and PVAFC20, the polyolefin fibres present helped in holding the fractured parts together. The steel fibre reinforced concrete slabs (SFC10 & SFC20) showed significantly superior performance in terms of multiple cracking and shear cone formation and slab integrity after impact. Typical crack patterns of slabs containing 2% volume fraction of fibres is shown in Fig. 6.

In the case of polyolefin fibre concrete slabs, the projectile perforated the slab containing 0.5% of polyolefin fibres. As the volume fraction is increased from 0.5% to 1% and 2%, an improvement in the resistance against projectile perforation was observed. Also the shear plug formed after impact was not dislodged from the bottom surface of the slab. The number of cracks and widths of cracks present after impact were reduced at the top and bottom surfaces of the slab containing 2% fibres. The other slabs with less fibres suffered more damage with excessive slab deformation. There is no clear difference in the final failure mode when slabs POFC05 and POFC10 were compared with the PC slab. Undoubtedly, there is an improvement in the case of slab POFC20 in terms of integrity after failure. The failure of fibres at the fracture zones were due to both pull-out and rupture.

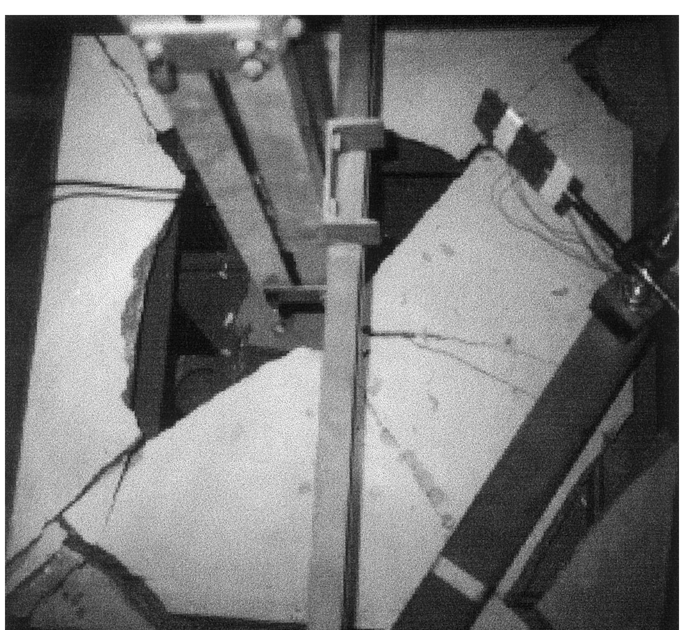

Fig. 4. Failure of plain concrete slab.

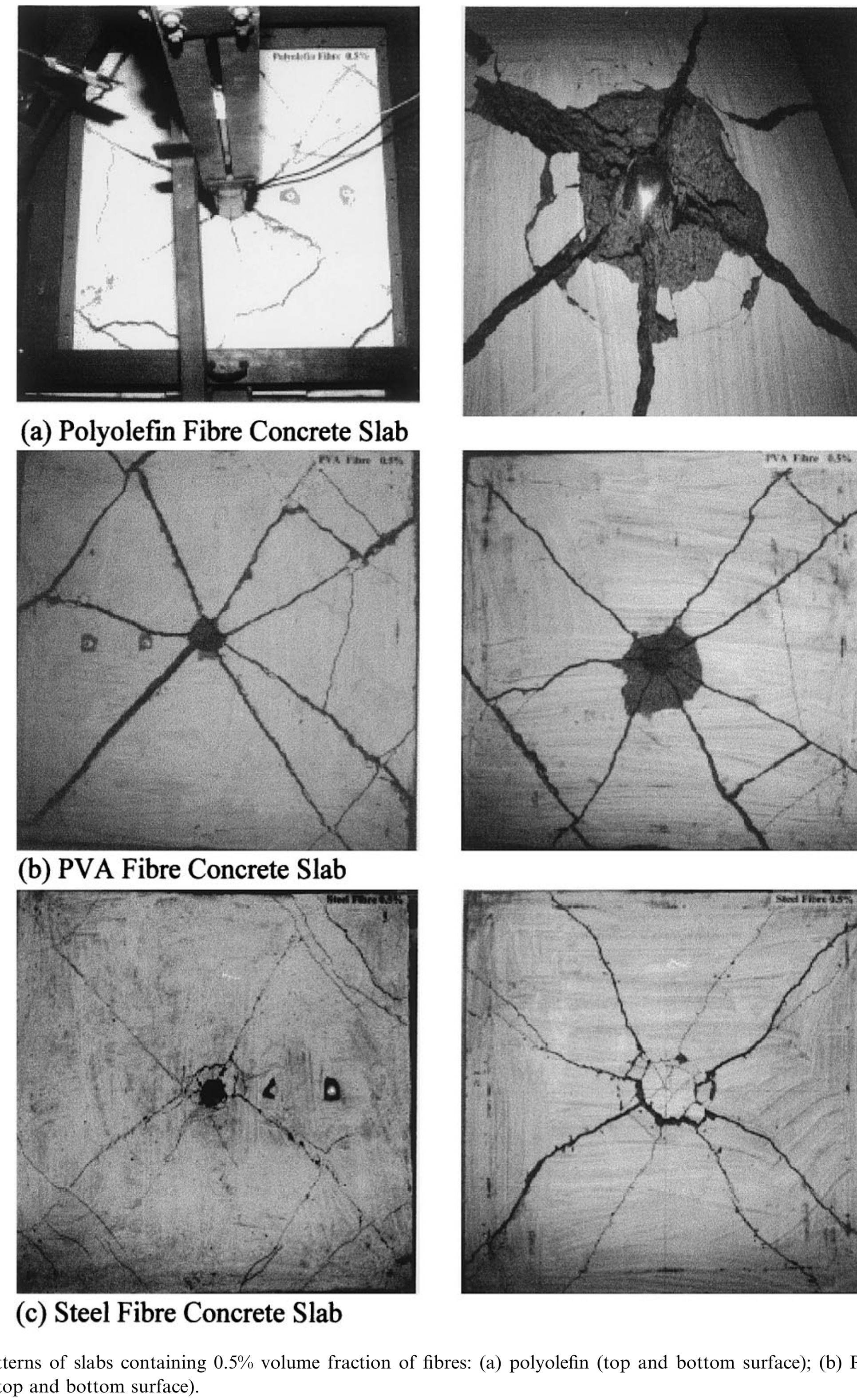

Fig. 5. Failure patterns of slabs containing 0.5% volume fraction of fibres: (a) polyolefin (top and bottom surface); (b) PVA (top and bottom surface); (c) steel (top and bottom surface).

A comparison of the failure patterns of slabs with polyvinyl alcohol (PVA) fibres showed that the slab with 0.5% fibres exhibited more cracks and failed by breaking into many pieces. As the volume fraction of fibres was increased from 0.5% to 1% and 2%, the number of cracks and the size of the failure zone were found to decrease reflecting a more localised failure. It may be observed that the slab containing 2% fibres failed into

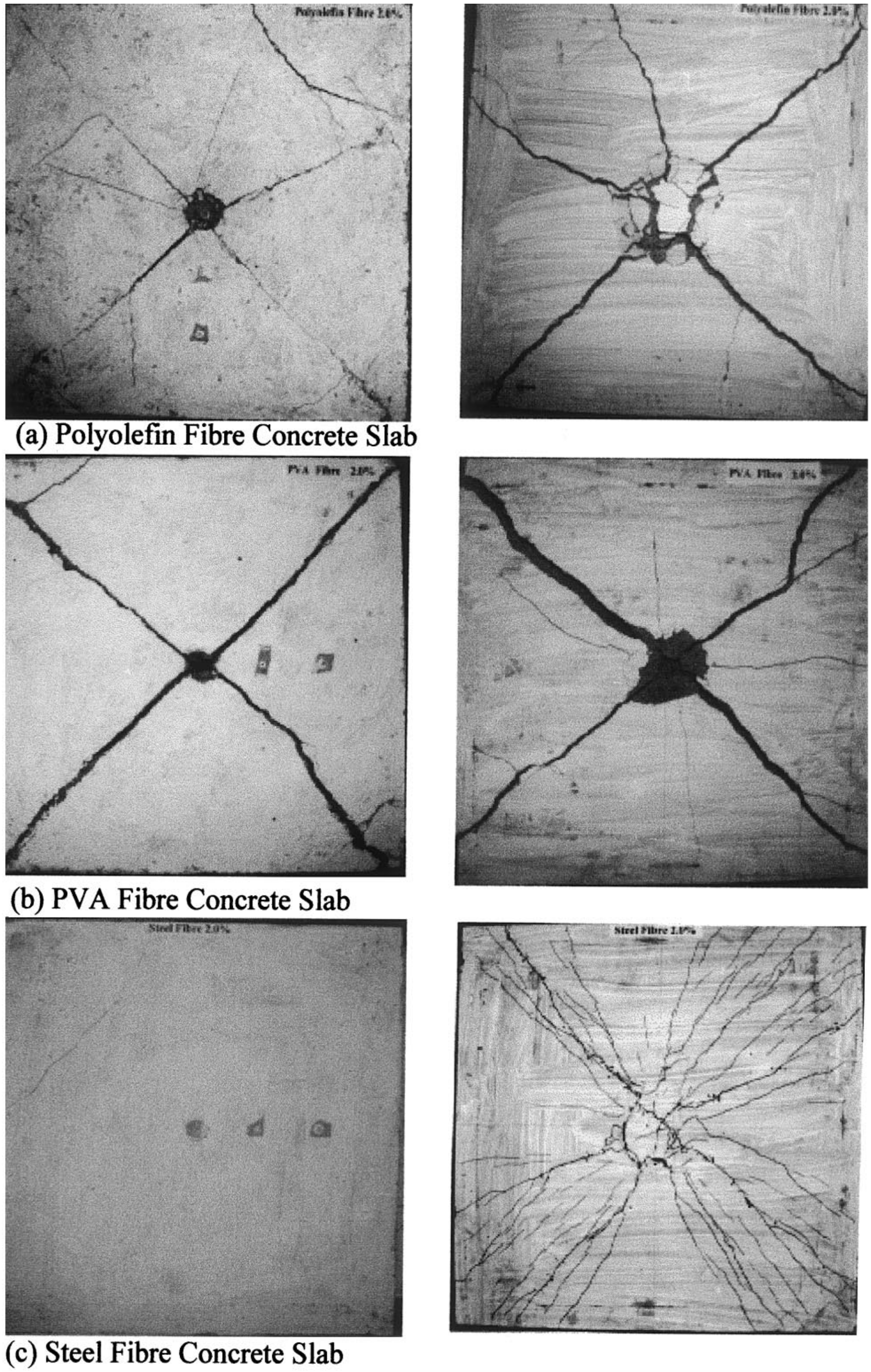

Fig. 6. Failure patterns of slabs containing 2% volume fraction of fibres: (a) polyolefin (top and bottom surface); (b) PVA (top and bottom surface); (c) steel (top and bottom surface).

four pieces, but, maintained the integrity within the broken pieces. The projectile perforated all the slabs reinforced with PVA fibres, and the fibres failed due to pull-out at the fracture zone.

The addition of steel fibres to concrete slabs resulted in considerable improvement in the impact resistance when compared to slab without fibres. Increasing the fibre content led to an increase in the number of cracks at the bottom face and a reduction in the width of cracks formed. The slab with 0.5% steel fibres failed due to the formation of a shear plug together with radial cracks emanating from the centre towards the corners. The size of the shear plug was reduced as the volume fraction of fibres added was increased from 0.5% to 1% and 2%. The residual displacement of the slab was 24.5 mm, 12.5 mm and 4.3 mm for the slab containing 0.5%, 1% and 2% volume fraction of fibres, respectively. This translates into an effective increase in stiffness and decrease in the degree of damage upon failure of the slabs with the addition of steel fibres. There were no cracks observed at the top surface of the slab as the steel fibre content was increased to 2%. The fibres failed due to pull-out at the fractured surfaces of the slabs.

In general, the failure pattern of the slabs was characterised by the formation of a frustum-shaped fracture zone followed by the formation of flexural cracks emanating from the centre towards the corners of the slab. Steel fibre concrete slabs showed better performance in terms of cracking behaviour, size of shear plug formed at failure and integrity of the slab at failure when compared to slabs reinforced with polyolefin or PVA fibres. Polyolefin fibres failed due to both pull-out and rupture, whereas, PVA and steel fibres failed by pull-out only along the fracture surfaces.

4.2. Load and displacement history characteristics

Fig. 7 shows the observed load history of PC slab along with the inertial load history. A major part of the initial peak in the observed load–time trace was due to the inertial load and it was similar to the force caused by rigid-body acceleration of the specimen from the at rest position close to the impact velocity of the projectile. The inertial load was calculated using Eq. (1) as explained previously. From Fig. 7 it was noted that the inertial load was about 90% of the observed peak load. If this large amount of inertial load is not corrected for,

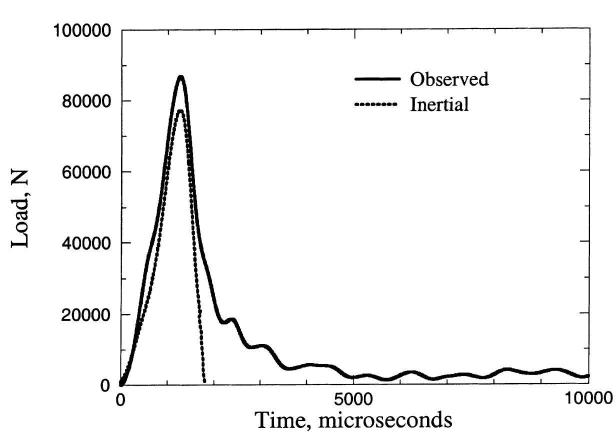

Fig. 7. Load vs time plot for plain concrete slab.

it would lead to erroneous values of energy calculations especially when these values are to be compared with static energy absorption values or with energy values obtained at different strain rates. It was observed that the inertial contribution was only significant during the initial stages of impact and its effect dissipates soon after.

Upon impact, the slab experienced a rapid increase in the load giving rise to the maximum load. This sudden increase in load to the maximum value occurs within 1 ms for all the slabs tested. The multiple contacts between the slab and the projectile was characterised by the occurrence of multiple peaks, referred as 'secondary peaks', in the observed load history. The peak loads may be influenced by various parameters, such as, contact velocity, mass of the projectile, nose shape of projectile, target thickness, target stiffness, concrete strength, roughness of the slab surface, boundary conditions of the slab, etc. However, in the present study, the above parameters did not vary significantly between specimens and hence did not affect the peak load measured. For the slabs tested the peak load was affected mainly by the nature of penetration of the projectile into the slab and the type and volume fraction of fibres used. A typical observed load history and displacement history of slabs reinforced with 2% fibres is shown in Fig. 8.

From the observed load history and displacement history of slabs containing 0.5% fibres, it was seen that slab PVA05 resisted higher loads than slab POFC05, whereas, slab SFC05 resisted higher loads than slab PVA05. This is true even for the slabs with 1% and 2% volume fraction of fibres. The duration of impact was about the same for slabs POFC05 and PVA05, while, that for slab SFC05 was about 3 times longer than the other slabs. The initial displacement rate was about the same for all the slabs tested.

In the slabs containing polyolefin fibres, a marginal increase in the first peak load was observed as the fibre content was increased. A considerable increase in the magnitude of the secondary peaks was observed when the fibre content was increased from 0.5% to 2%. The duration of impact was prolonged by the addition of fibres, about 10, 13 and 15 ms for the slabs with 0.5%, 1% and 2% of polyolefin fibres, respectively.

For slabs reinforced with PVA fibres, slab PVAFC20 resisted higher loads for a longer time duration. The duration of impact was about 9.5, 11.5 and 20 ms for slabs with 0.5%, 1% and 2% of PVA fibres, respectively. The impact duration was about 2 times longer for slab with 2% fibres compared to the slab with 0.5% fibres.

An increase in the peak loads, reduction in the maximum displacement and reduction in duration of impact experienced was generally observed as the volume fraction of steel fibres was increased. This indicates a stiffer response against impact with less damage caused

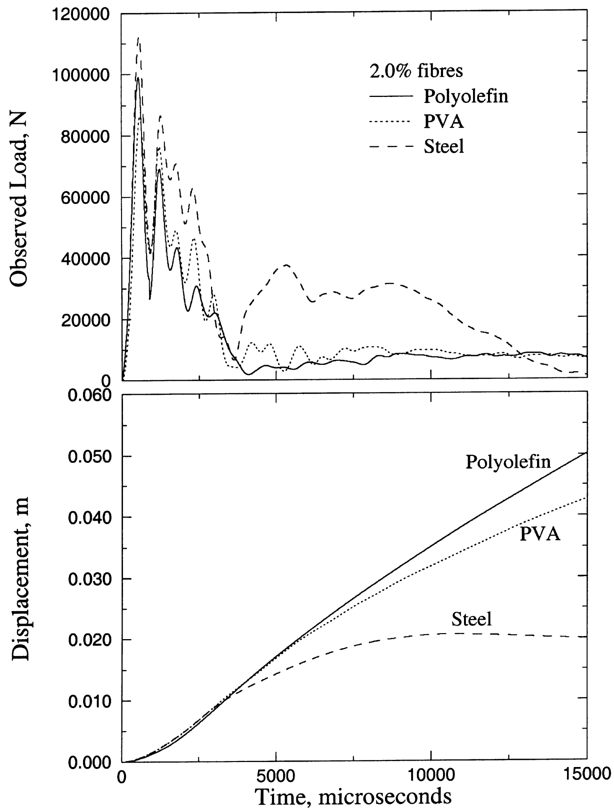

Fig. 8. Effect of fibre type on the observed load vs time and displacement vs time curves at 2% volume fraction of fibres.

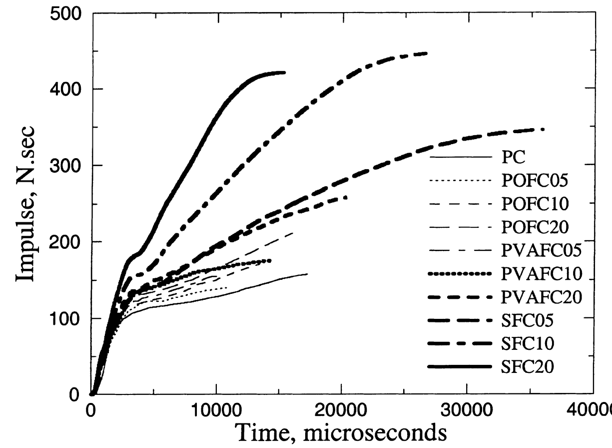

Fig. 9. Effect of V_f and fibre type on the impulse vs time curves.

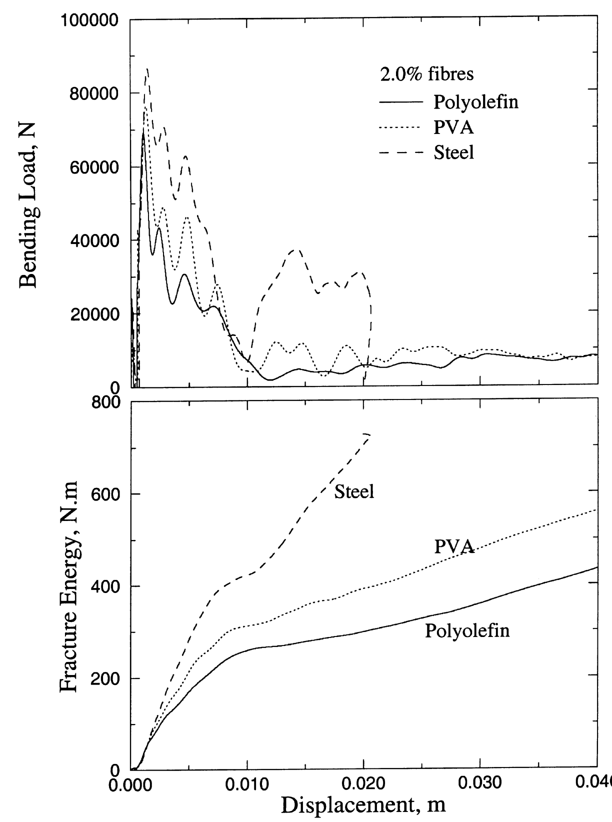

Fig. 10. Variation of bending load and fracture energy with displacement for slabs reinforced with 2% volume fraction of fibres.

to the slabs. The maximum displacement was reduced by about 36% and 56% when the volume fraction of steel fibres was increased from 0.5% to 1% and 2%, respectively. The reduction in the duration of impact was about 50% for 2% fibres (SFC20) compared to 0.5% fibres (SFC05).

From the impulse–time plots of the tested slabs (Fig. 9), it may be seen that slabs with steel fibres were subjected to higher impulse occurring over a shorter duration of time in the present study. The slabs with PVA fibres had impulse values less than that of steel fibre concrete slabs, but, the values were greater than those experienced by slabs with polyolefin fibres. At 2% fibre content, slab SFC20 showed 2 times higher impulse when compared to slab POFC20 whereas, slab PVAFC20 showed an increase of about 25% in the impulse when compared to slab POFC20.

4.3. Energy absorption characteristics

Fig. 10 shows typical bending load and fracture energy values plotted against displacement for slabs containing 2% volume fraction of fibres. The bending load was calculated using Eq. (2) after making the inertial correction to the observed load and the fracture energy was obtained using Eq. (6). For the same volume fraction of fibres, it was found that steel fibre concrete slabs resisted higher loads resulting in higher fracture energy values than slabs containing polymeric fibres. For the latter type of slabs tested, slabs containing PVA fibres absorbed more energy than those containing polyolefin fibres for the same volume fraction. In general, for any type of fibre examined, there was increase in the bending loads and fracture energy with increase in the volume fraction of fibres.

Based on the results of the present study, the fracture energy of the various slabs up to a displacement of 20 mm was used for comparison. The corresponding values for the observed load and bending load are reported in Table 3 and are also shown in Fig. 11. For 0.5% volume fraction of fibres, the slab with polyolefin fibres absorbed about 1.6 times energy (based on the bending load) as that absorbed by PC slab, whereas, the slabs with PVA fibres and steel fibres absorbed about 1.8 and 2.2 times that absorbed by PC slab. Increasing the volume fraction of fibres to 1%, POFC10 had a fracture energy value of 246.04 N m., which is 59% higher when compared to PC, while, PVAFC10 and SFC10 showed 2.1 and 3.2 times the fracture energy, respectively, that of plain concrete slab. The increase in fracture energy of slabs with 2% fibres compared to plain concrete slab was about 93%, 153% and 356% for slabs POFC20, PVAFC20 and SFC20, respectively.

Slabs reinforced with 0.5% and 1% polyolefin fibres had about the same energy absorption while a 21% increase in fracture energy was noted when the volume fraction of fibres was increased to 2%. An increase in the energy absorption capacities of 14% and 38% was observed, when the volume fraction of PVA fibres was increased from 0.5% to 1% and from 1% to 2%, respectively. In the case of slabs containing steel fibres, slab SFC10 had 1.5 times the fracture energy compared to SFC05 and SFC20 had 1.4 times the fracture energy compared to SFC10.

Similar observations could also be made for the fracture energy plots obtained using the observed load. As mentioned earlier, the fracture energy obtained after making the inertial correction to the observed load should be used when comparing with fracture energy values obtained at different strain rates. This would provide a proper representation of performance of the material subjected to high rate of loading.

Table 3
Fracture energy values based on observed and bending loads

Slab designation	Fracture energy (N m)	
	Using observed load	Using bending load
PC	240.89	154.40
POFC05	275.37	240.99
POFC10	288.61	246.04
POFC20	326.50	297.95
PVAFC05	327.03	283.20
PVAFC10	358.41	321.95
PVAFC20	426.39	391.34
SFC05	372.47	336.42
SFC10	538.42	493.02
SFC20	750.77	703.58

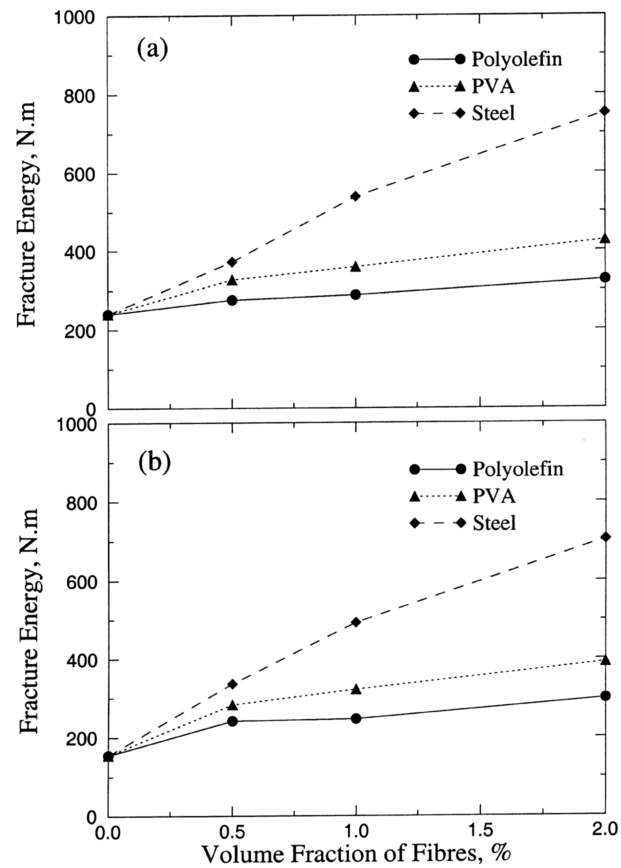

Fig. 11. Effect of V_f and fibre type on the fracture energy: (a) fracture energy by observed load; (b) fracture energy by bending load.

5. Conclusions

Steel fibre concrete slabs showed superior performance in terms of cracking characteristics, resistance to shear plug formation, energy absorption and integrity upon impact when compared to slabs reinforced with polyolefin and PVA fibres. Considering up to 20 mm displacement, at 0.5%, 1% and 2% volume fraction of fibres the steel fibre concrete slabs had about 40%, 100% and 136% higher fracture energy values, respectively, compared to polyolefin fibre concrete slabs, while about 19%, 53% and 80% higher fracture energy values, respectively, compared PVA fibre concrete slabs. It was also seen that the energy absorption capacities of PVA fibre concrete slabs were higher than the polyolefin fibre concrete slabs for the same volume fraction. The slabs with 0.5%, 1% and 2% volume fraction of PVA fibres had fracture energy higher by about 18%, 31% and 31%, respectively, compared to polyolefin fibre concrete slabs.

Polyolefin fibres failed by both pull-out and rupture, whereas, PVA and steel fibres failed by pull-out alone.

References

[1] Banthia N, Bentur A, Mufti A, editors. Fiber reinforced concrete: Present and future, Canadian Society for Civil Engineering, October 1998.

[2] ACI Committee 544. Design considerations for steel fiber reinforced concrete. ACI Structural Journal 1988;85(5):563–580.

[3] Bentur A, Mindess S. Fibre Reinforced Cementitious Composites. UK: Elsevier, 1990.

[4] Balaguru PN, Shah SP. Fibre-Reinforced Cement Composites. New York: McGraw-Hill, 1992.

[5] Struck W, Voggenreiter W. Examples of impact and impulsive loading in the field of civil engineering. Materials and Structures 1975;8(44):81–7.

[6] ACI Committee 544. Measurement of properties of fiber reinforced concrete. ACI Materials Journal 1988;November–December:583–93.

[7] Ramakrishnan V, Brandshaug I, Coyle WV, Schrader EK. A comparative evaluation of concrete reinforced with straight steel fibers and fibers with deformed ends glued together into bundles. ACI Journal 1980;May–June:135–43.

[8] Swamy RN, Jojagha AH. Impact resistance of steel fibre reinforced lightweight concrete. The International Journal of Cement Composites and Lightweight Concrete 1982;44(November)209–220.

[9] Radomski W. Application of the rotating impact machine for testing fibre-reinforced concrete. The International Journal of Cement Composites and Lightweight Concrete 1981;3(1):3–12.

[10] Reinhardt HW, Kormelig HA, Zielinski AJ. The split Hopkinson bar, a versatile tool for the impact testing of concrete. Materials and Structures RILEM 1986;19(109):55–63.

[11] Malvern LE, Tang T, Jenkins DA, Gong JC. Dynamic compressive strength of cementitious materials. In: Cement Based Composites: Strain Rate Effects on Fracture. Materials Research Society Symposia Proceedings 1986;64:119–38.

[12] Krenchel H. Fiber reinforced brittle matrix materials. In: Fiber Reinforced Concrete. SP-44. ACI Publication 1974:45–77.

[13] Johnston CD. Steel fiber reinforced mortar and concrete: a review of mechanical properties. In: Fiber Reinforced Concrete. SP-44. ACI Publication 1974:127–42.

[14] Gopalaratnam VS, Shah SP, John R. A modified instrumented charpy test for cement-based composites. Experimental Mechanics 1984;24(2):102–11.

[15] Ito C, Ohnuma H, Nomachi SG, Residual strength of PC beam after subjected to impact load. In: Proceedings of the 28th Japan Congress on Materials Research 1985;March:165–68.

[16] Naaman AE, Gopalaratnam VS. Impact properties of steel fibre reinforced concrete in bending. The International Journal of Cement Composites and Lightweight Concrete 1983;5(4):225–33.

[17] Bentur A, Mindess S, Banthia N. The behaviour of concrete under impact loading: experimental procedures and method of analysis. Materiaux et constructions 1986;19(113):371–8.

[18] Suaris W, Shah SP. Properties of concrete subjected to impact. Journal of Structural Engineering 1983;109(7):1727–41.

[19] John R, Shah SP. Constitutive modelling of concrete under impact loading. In: Proceedings of the First International Conference on Effects of Fast Transient Loadings. Lausanne 1987;August:37–65.

[20] Banthia NP, Impact resistance of concrete. PhD thesis, University of British Columbia. Vancouver (British Columbia, Canada), 1987.

[21] Banthia N, Mindess S, Bentur A, Pigeon M. Impact testing of concrete using a drop-weight impact machine. Experimental Mechanics 1989;29(1):63–9.

[22] Banthia N, Yan C, Sakai K. Impact resistance of concrete plates reinforced with a fiber reinforced plastic grid. ACI Materials Journal 1998;95(1):11–8.

[23] Suaris W, Shah SP. Inertial effects in the instrumented impact testing of cementitious composites. Cement Concrete and Aggregates ASTM 1981;3:77–83.

[24] Timoshenko S, Woinowsky SSK. Theory of Plates and Shells. New York: McGraw-Hill, 1959.

[25] Jawad MH. Theory and Design of Plate and Shell Structures. New York: Chapman & Hall, 1994.

[26] Basheerkhan M. Impact behaviour of fibre reinforced cement concrete composite slabs. PhD thesis, National University of Singapore. Singapore, 1999.